

Article

# Planing Hull Hydrodynamic Performance Prediction Using LincoSim Virtual Towing Tank

Ermina Begovic <sup>1,\*</sup> , Carlo Bertorello <sup>1</sup> , Raffaele Ponzini <sup>2</sup>  and Francesco Salvatore <sup>3</sup>

<sup>1</sup> Department of Industrial Engineering, University of Naples Federico II, Via Claudio 21, 80125 Napoli, Italy; bertorel@unina.it

<sup>2</sup> HPC Department, CINECA, Milan Office, Corso Garibaldi, 86 Milano, 20121 Milan, Italy; r.ponzini@cineca.it

<sup>3</sup> HPC Department, CINECA, Rome Office, Cineca, Via dei Tizii 6/B, 00185 Rome, Italy; f.salvadore@cineca.it

\* Correspondence: begovic@unina.it

**Abstract:** This work shows the performance of LincoSim, a web-based virtual towing tank enabling automated and standardized calm water computational fluid dynamics (CFD) data sampling, extending previous published applications to the case of a high-speed hull. The calculations are performed for a 1:10 scale model of a 43 ft powerboat hull form in the Froude number range from 0.3 to 2.0. The counterpart physical model is the experimental fluid dynamics (EFD) campaign performed at the University of Naples Federico II, where the resistance, sinkage and trim data have been measured. The EFD/CFD data comparison is performed and shown with a discussion of the spotted differences. The average percentage differences between the EFD and CFD data for the whole speed range are 1.84, 6.87 and 6.94 for the resistance, dynamic trim, and sinkage, respectively. These results confirm the maturity of the standardized and automated CFD modeling for calm water hydrodynamic analysis included in LincoSim, even at very high Froude numbers. The wetted length of the keel and chine and the wetted surface are calculated from numerical data using the advanced post-processing. Finally, as a work in progress, we test a first comparison for the same hull of the EFD and CFD data, considering two seakeeping conditions for head waves at a given wavelength for two velocity conditions. Also, this kind of analysis confirms the tight correlation between the measured and computed outcomes. This synergic interplay of EFD and CFD can link the advantages of both methods to support hull design but also requires experiment planning and final data analysis to obtain physical parameters not easily measurable in laboratory, such as the wetted surface, wetted lengths, proper viscous contribution, and pressure distribution both in calm water and in waves.

**Keywords:** CFD; EFD; standardized CFD workflow; planing hull; resistance in calm water; seakeeping



**Citation:** Begovic, E.; Bertorello, C.; Ponzini, R.; Salvatore, F. Planing Hull Hydrodynamic Performance Prediction Using LincoSim Virtual Towing Tank. *J. Mar. Sci. Eng.* **2024**, *12*, 794. <https://doi.org/10.3390/jmse12050794>

Academic Editor: Kostas Belibassakis

Received: 16 April 2024

Revised: 1 May 2024

Accepted: 3 May 2024

Published: 9 May 2024



**Copyright:** © 2024 by the authors. Licensee MDPI, Basel, Switzerland. This article is an open access article distributed under the terms and conditions of the Creative Commons Attribution (CC BY) license (<https://creativecommons.org/licenses/by/4.0/>).

## 1. Introduction

During the last few years, the computational fluid dynamics (CFD) technique has become a “standard” tool for addressing calm water resistance prediction and studying complex phenomena such as the planing regime of small crafts, characterized by the dynamic trim, flow separation at chine, pressure wetted area and whisker spray area. Remarkable reproduction of the experimental data from the numerical towing tank has been reported by [1–4]. Ref. [5] provided a review of the most recent works on high-speed planing hulls and, for a selected hull in a Froude number  $Fr$  range from 1.14 to 2.50, performed a calculation of the numerical uncertainty of the resistance, trim and sinkage.

However, CFD modeling of planing hulls requires expert users to decide on different moving mesh techniques (overset/chimera and morphing grid), turbulence models, domain boundaries, and convergence criteria to arrive at a numerical set-up that will provide reliable results.

In [6] an automatic and web-based application of a virtual towing tank named LincoSim specifically designed to perform automatic CFD modeling of hydrodynamic performances in calm water was presented. The tool uses only open-source software and

deploys high-performance computing infrastructures to take advantage of well-established technological bricks. Validation and verification of the LincoSim has been performed in [7] for the planing hull systematic series by [8], showing how the same standardized workflow for all the tested hulls at each velocity condition was effective. The work showed clearly that if the mesh is topologically standardized, then the stopping criteria and the solver setup are coherent, allowing for safe data comparison of different hulls under different flow conditions. In [9] the same approach was tested using a catamaran experimental dataset including the hull dynamics, resistance, and wave pattern measurements. The main outcome was that the standardized and automated CFD workflow proposed in LincoSim was also suitable for the selected multi-hull case.

Today, with the increased computational capabilities and cloud computing, the implementation of the automatic CFD modeling concept can be proposed at a larger scale. Low-fidelity methods, such as the Savitsky method [10] or regression analysis, are extremely fast, based on the assumptions of the prismatic hull form and pure planing condition, and are those widely used in the design stage. In these first steps, completely automatic CFD modeling could be of particular interest for non-expert CFD users who can be assisted by the platform to obtain reliable results and correct trends of hydrodynamic properties when considering hull form modifications and optimization.

Seakeeping of the planing hull in designer practice is often limited to the calculation of the vertical accelerations at the center of gravity and bow, as they are the input for structure scantling and added resistance in waves, according to the regression formula developed by [11,12]. Even though mathematical models developed according to [13–15] have proven validity for the prediction of prismatic hulls, their use is still limited to the research groups, not to the designer communities. The experimental results of the recent systematic series [16–18] are available, but they are often limited to their ranges and provide as the final result the statistical distribution for accelerations.

Today, seakeeping CFD simulations for planing hulls are limited to regular waves and they offer an extremely valid tool for the impact analysis, but the complexity of the numerical setting and required computational time are still limiting factors. Anyway, wave/hull interaction CFD modeling is still an open point in research, especially when considering the usage of open-source libraries. The limited validation dataset availability represents a concrete limitation of the definition of a standardized workflow. Even if under development, a LincoSim seakeeping workflow has been proposed specifically for a research project (e-SHyIPS, see <https://www.e-shyips.com> (accessed on 15 February 2024), still based on the OpenFOAM toolbox, following a robust methodology proposed by [19] to ensure the minimization of wave reflections using forcing zones. It is worthwhile to underline that the forcing zones were recently made available to the OpenFOAM community in version 11. The forcing zones follow the state-of-the-art principles outlined in [19] but have been implemented by CFD-Direct coherently with the evolution of the OpenFOAM toolbox.

This work shows the performance of the LincoSim web-platform for a high-speed hull, analyzing the suitability of the platform for a wider Froude number range with respect to what was already published in [7] and discussing what could be the future of the open libraries for the non-expert CFD users. The calculations in calm water are performed for the 1:10 scale model of a 43 ft hull form in the Froude number range 0.3–2.0. The hull form is the one studied in [20–23]. New tests have been performed at the University of Naples Federico II and the resistance, sinkage and trim have been measured. Thanks to CFD data's advanced post-processing, the values of the wetted length of the keel and chine are obtained to have a correct prediction of the full scale resistance, as well as the pressure distribution along the hull, showing possible design applications.

Furthermore, experiments and simulations at regular head wave at two different velocities are performed. In detail, the wavelength is selected so that  $\lambda/L = 3.56$  and the velocity conditions are specified to match the Froude number  $Fr$  values of 0.99 and 1.49, respectively. The numerical outcomes are compared side by side with the experimental

ones by performing the same processing for selected hull signal dynamics, looking at specific nonlinear behaviors related to the selected planing conditions.

## 2. LincoSim Web Platform

### 2.1. Simulations Set-Up in Calm Water

The web application named LincoSim, first developed in 2018 for the Horizon 2020 project LINCOLN (<http://www.lincolnproject.eu/>), (accessed 30 March 2024) has been refactorized and updated today to support early design analyses within the Horizon 2020 e-SHyIPS (<https://e-shyips.com/>), (accessed 15 February 2024) The e-SHyIPS project aims to define new guidelines for an effective introduction of hydrogen in the maritime passenger transport sector and to boost its adoption within the global and EU strategies for a clean and sustainable environment, toward the accomplishment of a zero-emission navigation scenario. With respect to the functionalities included into the LincoSim web application as available at the end of the LINCOLN project, several new functionalities have emerged as requirements to face the specific activities related to the e-SHyIPS project. The reason behind the necessity of adding new functionalities is strictly related to the signature of the e-SHyIPS project: the presence of H<sub>2</sub>-based propulsion systems. At the original stage, LincoSim only allowed calm water analysis to be performed, while, thanks to a recent re-design and re-factorization work, new functionalities are under development, also allowing for seakeeping analysis, thus including the presence of regular waves. If, in extreme synthesis, LincoSim was a suitable tool to obtain calm water data from 3D RANS CFD standardized and automated simulation for a given hull shape, the evolution also contains new functionalities such as hydrostatic analysis, stability analysis, and wave hull interaction. These tools open up the possibility of performing numbers of early design evaluations that are fully coherent with other more computationally expensive activities related to calm water and seakeeping simulations, avoiding any possible input-related misleading submission and opening up the possibility for designers to take advantage of complex technologies without any specific competences other than the ones related to the physics of the problem under consideration.

Figure 1 reports the types of simulations developed within the LincoSim platform: hydrostatics/stability, calm water, and seakeeping simulations. Seakeeping simulations, i.e., wave-hull interaction, present automation challenges and their implementations within the LincoSim are still ongoing. For this reason, the simulations were performed using a standardized workflow by means of a command line interface (CLI) instead of using the LincoSim web interface as was possible for the calm water simulations.

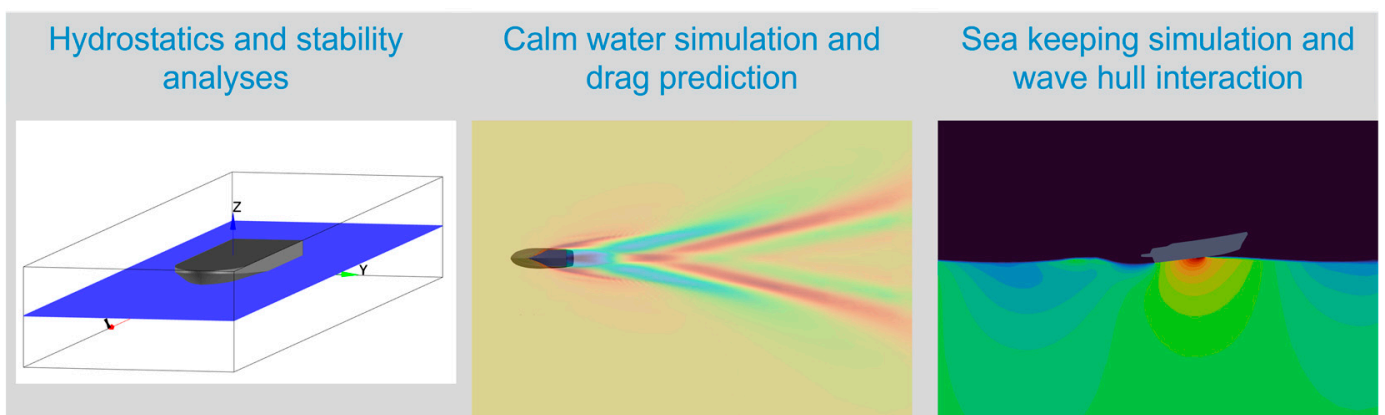


**Figure 1.** LincoSim modules: hydrostatic and stability analyses (**left**), calm-water simulations (**middle**), and seakeeping simulations (**right**).

The standardization of the calm water CFD modeling is based on the physics of the problem that defines the computational domain and the mesh cell sizes according to a given

standard mesh topology. See [6,7] for more CFD settings and modeling details. In Figure 2, the domain sizes and the mesh topology are shown for the P43 power boat geometry, which is considered in the present work.

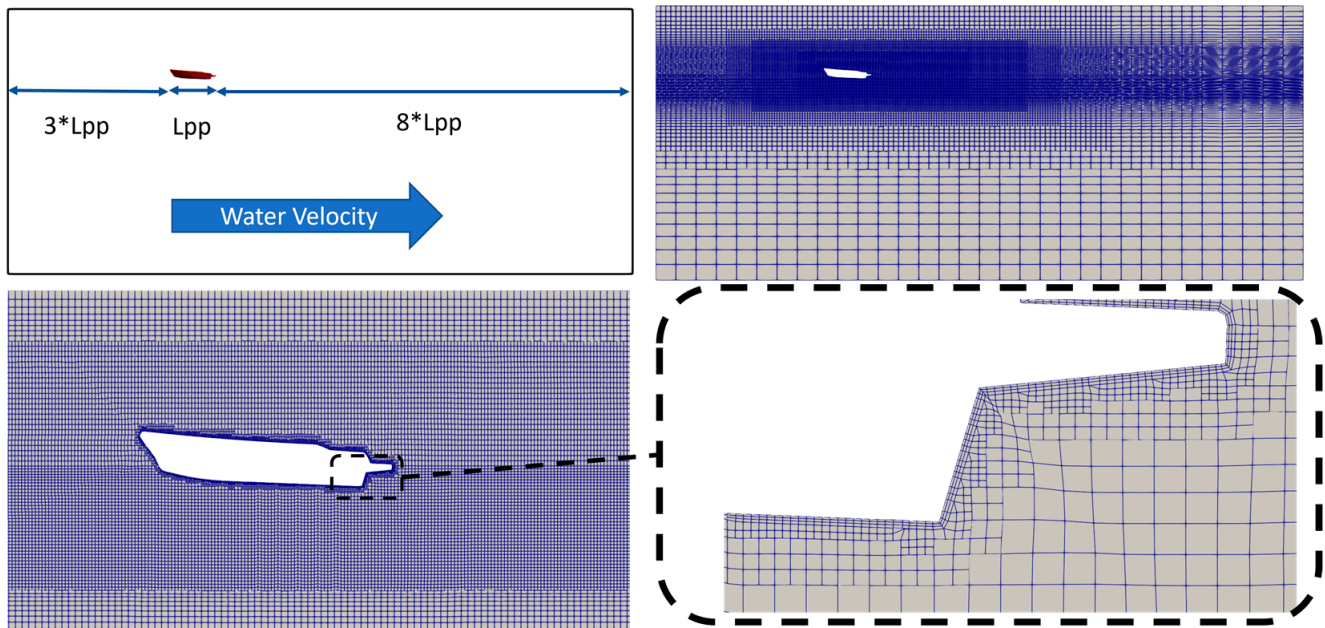


**Figure 2.** Domain extensions and mesh topology for the P43 hull at  $Fr = 1.392$ .

The hull length is used to define the domain extent, as shown in Figure 2 in the top left box and the mesh refinements boxes positioning, while the hull speed is used to define the near wall cell height targeting a dimensionless wall distance ( $y^+$ ) value of about 100; similar settings have been proposed more recently by [24]. The turbulence model selected is the SST  $k-\omega$ , see [25], which is recognized to be effective in the marine field of application. Standard wall functions are applied. The time step is fixed and is set to ensure, for the given nominal hull velocity, a Courant number value lower than unity. For the lower and higher Froude numbers, the value of the time step is set to 0.00372 s and 0.000165 s, respectively. The CFD model is solved using the interFoam solver as available from the OpenFOAM toolbox. The hull is studied by imposing a symmetry plane at the hull mid-section (half hull). Using this approach, the average mesh cell count is about two million. We underline that this approach has only been tested and validated for the model scale; nevertheless, considering the research applications for full-scale CFD models, like [26], we are looking forward to having a better understanding of its applicability for full-scale CFD modeling.

The proposed approach based on a meshing strategy tailored to satisfy the given mesh topology and requirements for each given velocity, thus adjusting the domain size, the mesh cells size and the boundary layer cells, has never been tested on a Froude number greater than 1.7. Therefore, this work, in which the Froude number ranges from 0.3 to 2.0, is a new validation, which is useful to assess the performance of the platform on a wider Froude number range.

## 2.2. Simulations Set-Up in Regular Waves

As discussed earlier, seakeeping simulation standardization is still ongoing; nevertheless, a Command Line Interface (CLI) tool to manage the workflow is operational and, with reduced manual intervention, can configure and run complete simulations.

For the simulations in regular waves, three degrees of freedom have been considered, namely:

- Heave motion defined by the hull VCG(t) coordinate variation compared to the averaged value;

- Pitch motion, given as the pitch rotation angle;
- Roll motion, given as the roll rotation angle.

All the simulations are performed in the hull reference system with the definition of heading corresponding to  $\beta = 0$  degrees for head waves. For the CFD modeling of this kind of problem, a set of good practice strategies according to [27] has been adapted:

The domain specifications are as follows:

- X-direction: five times the maximum between the wavelength and hull length
- Y-direction: same as the x-direction
- Z-direction: two times the maximum between the wavelength and hull length

The background mesh spacing specifications are as follows:

- X-direction: between 30 and 40 mesh cells per wavelength
- Y-direction: same as the x-direction
- Z-direction: between 10 and 15 mesh cells per wave amplitude

Additionally, the target mesh cell size on the hull is set to be equal to  $1/250$  of the hull length. The meshing strategy to achieve such goals includes vertical one-dimensional refinement, horizontal two-dimensional refinements in nested boxes and surface-based refining and layering. The OpenFOAM snappyHexMesh tool is used, thus realizing a full open-source-based CFD workflow.

Considering the requirements defined above, for a given hull shape, the mesh cell count increases when shifting from long-period to short-period waves. To increase the time to the result by taking advantage of the symmetric domain definition, head waves are treated as half domains with a symmetry plane in correspondence of the Y-axis. The resulting mesh size in our test case was about four million cells.

Also, the forcing zones and forcing parameter values have been set according to [27]. In Figure 3, an example of the forcing zone is shown. The general idea is to force the wave equations on an external frame, which is not too close to the hull position and let the solution of the Navier–Stokes equations adapt to the forced condition, transporting the wave into an internal frame directly surrounding the hull. A set of numerical parameters must be defined to simulate waves following such a kind of forcing zone approach: the most important ones are the frame extents, the forcing strength, and the spatial forcing shape function.

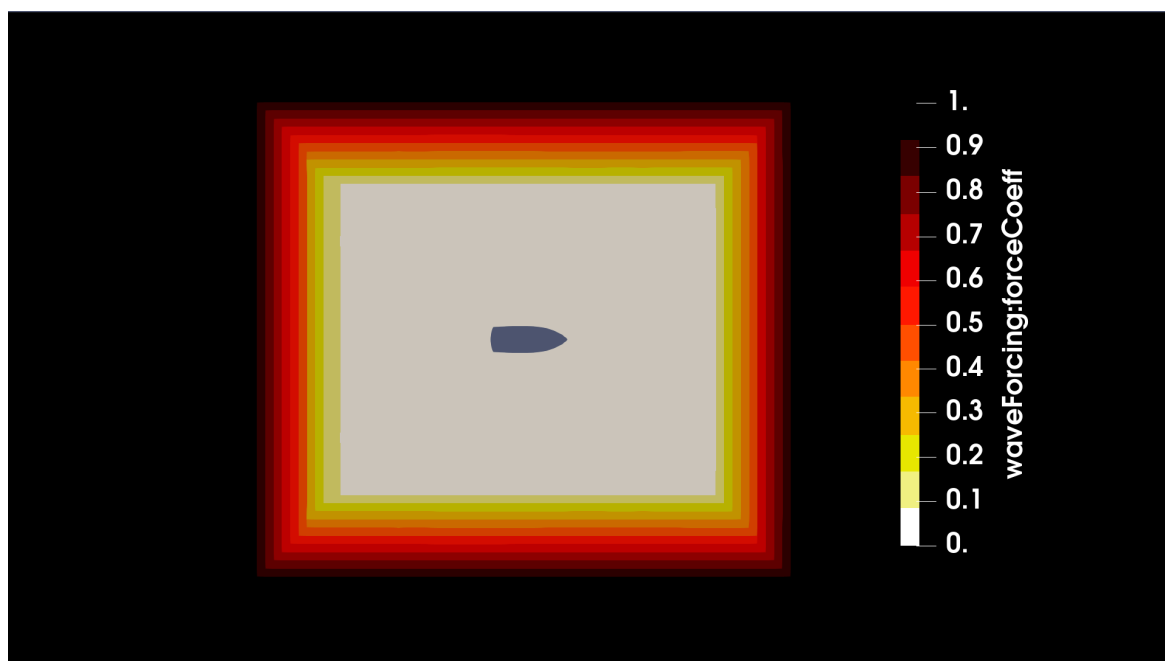


Figure 3. Example of a wave forcing zone.

According to [19] the frame extents are defined according to the imposed wave so that the internal (non-forced) frame extent is equal to 1 wavelength and the external (forced) frame extent is equal to 1.5 wavelengths. The forcing strength is defined by a parameter that is the inverse of a forcing time parameter  $\tau$ , which basically corresponds to the time needed to force the flow to the given wave form. Therefore,  $\tau$  can be as a first approximation set equal to the residence time of the flow within the force region, which can be expressed as the ratio between the forcing zone thickness and wave celerity. More accurately, the value has been selected in our simulations, again according to [27] using the code provided by the authors through a GitHub repository (see [28], accessed on 30 April 2024), which minimizes the wave reflections in the computational domain. In a few words, the auxiliary code optimizes the analytical predictions for the reflection coefficient for long-crested free-surface wave propagation when using relaxation zones as described in [27]. A useful manual is distributed along with the code (see [29] (accessed on 30 April 2024) with a general description of the released application and average suitable settings. The code contains recommendations on how to further tune the relaxation zone's parameters depending on the waves, including possible shape functions. In our models, we used the half cosine ramp function.

Moreover, it is worth noting that forcing can be imposed on selected velocity components and/or on the volume fraction. In OpenFOAM implementation, horizontal and vertical velocity components are forced alongside the volume fraction. Finally, according to the availability of regular wave models in OpenFOAM, we selected second-order Stokes wave modeling.

Following the indications of [27], the top and bottom planes are set as the free pressure and no-slip boundary, respectively. For the zero hull velocity simulations, all the vertical boundaries are set as wave equations, while for the non-zero hull velocity simulations, streamwise max e min vertical boundaries are set as the inflow and outflow conditions. To complete the model setup, we use a parametric simulation end-time value equal to 30 wave time periods ( $T$ ). This value has been considered sufficient to guarantee the onset of a periodic hull dynamics response to the incoming wave. The starting integration time step is set to be equal to 1/150 of the wave period and is automatically adjusted to ensure a value of the Courant number lower than or equal to one. This setting for the time integration step is considered the optimal theoretical value. During the simulation time evolution, we sampled several fluid dynamics and rigid body dynamics quantities. These data are necessary to be able to define relevant output parameters like:

- Incoming wave amplitude.
- Hull rigid body dynamics.
- Accelerations at given hull locations.

The requirement of also monitoring the signal of the incoming wave amplitude is related to the fact that the imposed input values are never reached due to numerical inaccuracies. As such, the effective wave height is measured from the corresponding simulation to evaluate the deviations from the imposed input amplitude and to improve the accuracy of the results where input amplitudes appear. Even if more accurate analysis and validation should be performed to assess the impact of numerical settings on wave signal losses in the non-forced zone, from what is observed so far with the present settings, the choices performed for the meshing and adaptive integration time step limit the wave signal loss, ensuring for more than 90% of the imposed wave signal at the hull reference location.

The qualitative outcomes are presented in Figure 4, where the pressure flow field distribution around the hull is shown over four successive time instants.

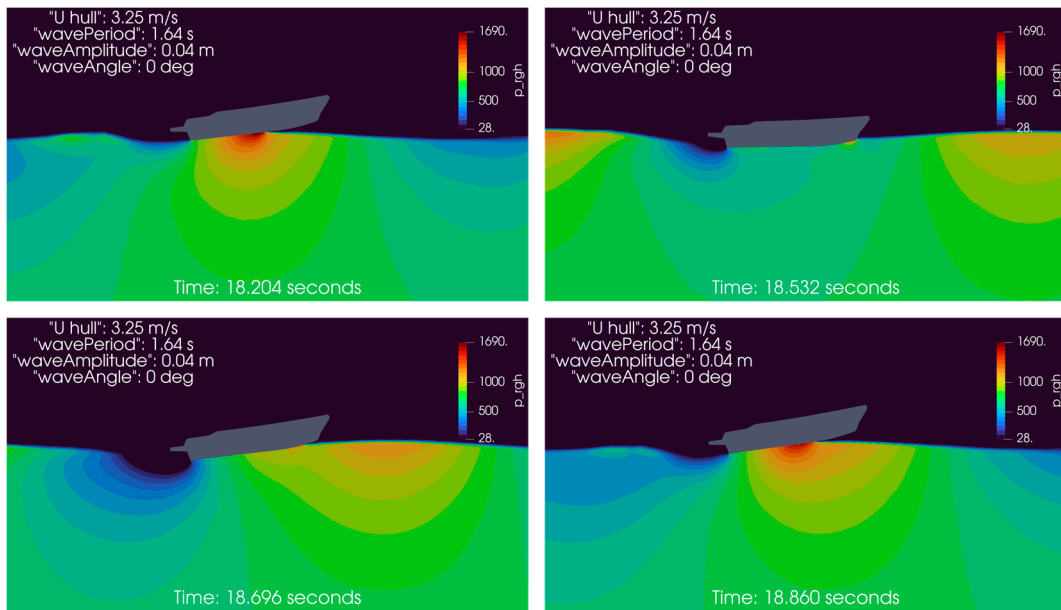


Figure 4. Pressure flow field over time.

### 3. Experimental Tests of P43 Powerboat

All the experiments have been performed in the towing tank of the University of Naples, Department of Industrial Engineering, whose dimensions are  $135 \times 9 \times 4.2$  m. The towing carriage speed ranges from 0.1 to 7 m/s. The P43 planing boat is a deep V hard chine form with a transom deadrise angle of 14 degrees up to 45 degrees at the bow, given in Figure 5. The 1:10 scale GRP built model, complete with the deck without appendages, was fixed to the carriage by the measurement instrument (metallic arm shown in Figure 5) at the position of  $X_{arm} = 0.278$  m from the transom, at the height of 0.08 m above the waterline. The model was free to pitch and to move along the vertical axis, but it was constrained for surge, sway, roll and yaw. The model's main characteristics are reported in Table 1.



Figure 5. Cont.

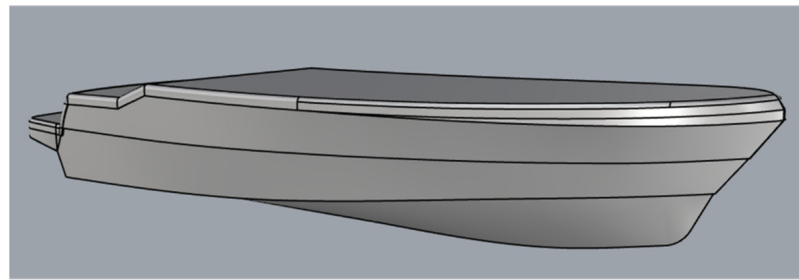


Figure 5. P43 planing hull model body plan from [23], in the towing tank and CAD model.

Table 1. Principal data of the P43 power boat.

$L_{M-OA}$ (m)	$B_C$ (m)	$B_{OA}$ (m)	$T_{AP}$ (m)	$m$ (kg)	Static Trim (deg)	$LCG_T$ (m)	$VCG_{BL}$ (m)	$r_{44-air}/B_C$ (-)	$r_{55r}/L_{OA}$ (-)
1.219	0.360	0.425	0.069	11.38	2.32	0.390	0.118	0.284	0.259

### 3.1. Resistance in Calm Water

The series of runs in calm water starting from the Froude number 0.3 up to 1.96 has been performed, measuring in each run: total resistance, sinkage at the X\_arm position and dynamic trim. The sampling frequency was 500 Hz. Uncertainty analysis of the measured values was performed using standard ITTC procedures. All data are reported in Table 2.

Table 2. Experimental results in calm water.

$V_M$ (m/s)	$Fr$ -	$R_T$ (N)	Running Trim $\tau$ (deg)	Sinkage (mm)	$U_{AR}$ %R	$U_{AT}$ % $\tau$	$U_{AS}$ %S
0.98	0.30	2.82	0.4	-4.97	1.0088	1.0050	0.1001
1.30	0.40	5.75	1.14	-11.62	1.0026	1.0001	0.1094
1.63	0.50	12.46	3.73	-21.6	1.0009	1.0001	0.1016
1.95	0.60	15.42	4.97	-21.74	1.0006	1.0000	0.1042
2.28	0.70	17.04	5.40	-13.84	1.0012	1.0000	0.1292
2.60	0.80	19.11	6.26	-9.12	1.0009	1.0000	0.1042
2.93	0.90	20.43	6.69	-1.25	1.0011	1.0000	0.4061
3.25	0.99	20.14	6.45	4.91	1.0006	1.0000	0.2141
3.58	1.09	19.59	5.95	13.13	1.0004	1.0000	0.1212
3.90	1.19	19.11	5.38	18.4	1.0009	1.0000	0.1102
4.23	1.29	18.94	4.81	23.6	1.0005	1.0000	0.1108
4.55	1.39	18.94	4.32	24.6	1.0022	1.0000	0.1438
4.88	1.49	19.04	3.91	24.4	1.0011	1.0000	0.1127
5.20	1.59	19.56	3.57	26.4	1.0007	1.0000	0.1200
5.52	1.69	20.38	3.28	28.1	1.0011	1.0000	0.1505
5.83	1.78	21.26	3.00	28.1	1.0014	1.0001	0.1326
6.16	1.89	22.16	2.83	30.2	1.0025	1.0001	0.1455
6.49	1.96	23.44	2.63	31.1	1.0032	1.0003	0.1569

### 3.2. Seakeeping in Regular Wave

The seakeeping behavior of the P43 hull has been extensively analyzed in [21] for the ship having 30% more displacement and in [23] at 4 velocities in irregular head waves. For the purpose of the first seakeeping calculations by LincOSim, only two tests in regular wave have been performed at two speeds, 3.25 m/s and 4.87 m/s, corresponding to 20 and 30 knots in ship scale, the same as the ones used in previous works. The experiments performed for this research are only for the wavelength where the resonance occur  $\lambda/L = 3.557$  and wave amplitude is 44 mm.

The model has been additionally equipped with two accelerometers, one at 0.47 m and one at the bow at the position of 1.09 m from the transom. All the experimental data (both

calm water and seakeeping conditions) are measured with heave at the position of  $X_{arm}$  for physical setup requirements and are then recalculated for the  $LCG$  reference position in order to be compared to the CFD simulations data that are instead directly monitored at the  $LCG$  location.

#### 4. Results Comparison

##### 4.1. Measured vs. Calculated Results in Calm Water

The simplest analysis of data is the direct comparison of the measured total resistance, sinkage and trim. The measured and calculated data have been reported in Figures 6–8. The experimental uncertainty is around 1% for resistance and dynamic trim and 0.5% for sinkage. The error bars are drawn inside the markers of experimental data.

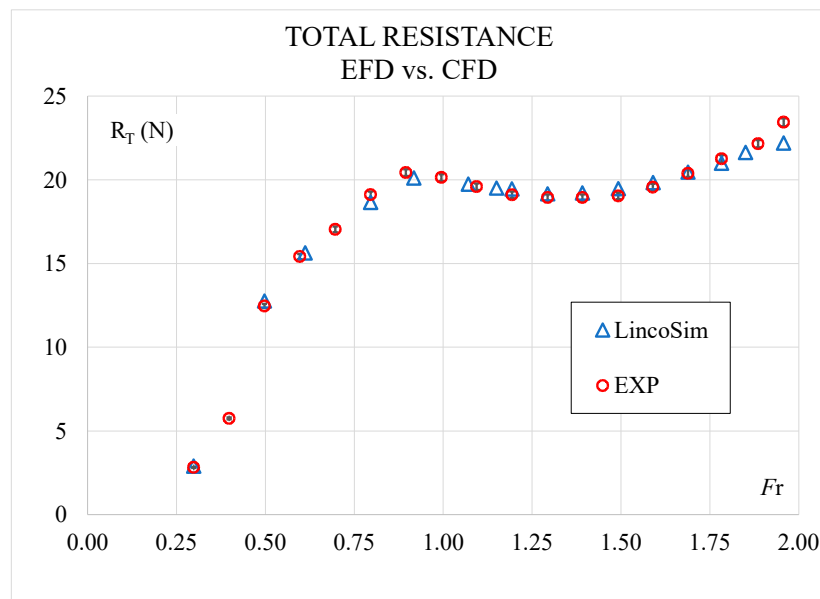


Figure 6. Total resistance comparison.

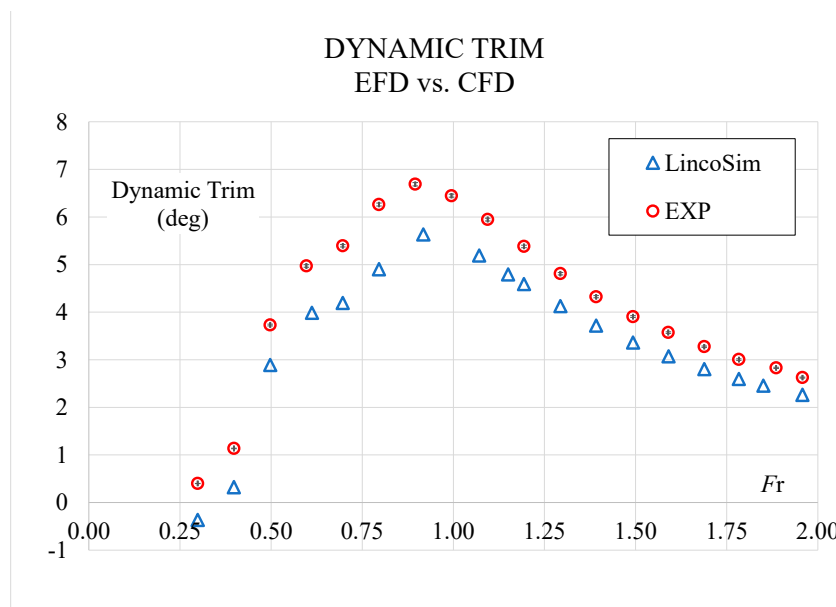
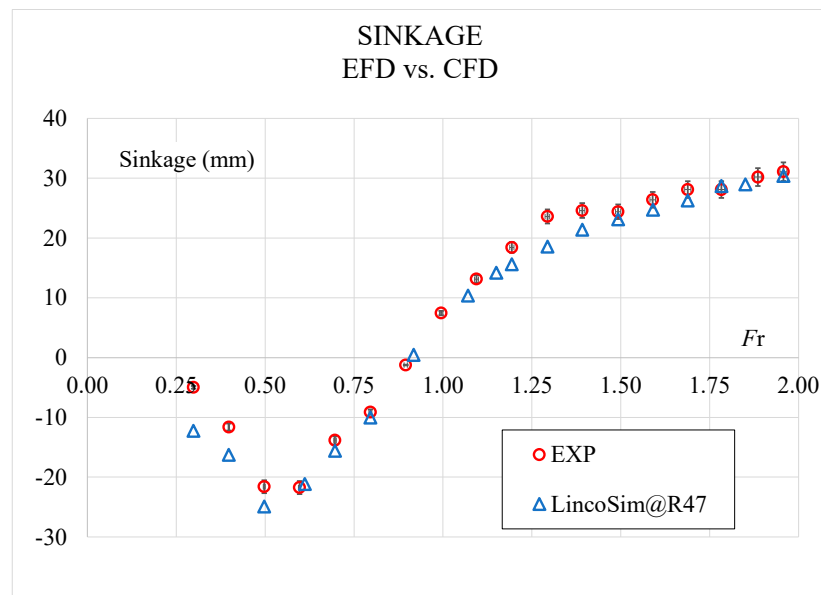


Figure 7. Dynamic trim comparison.



**Figure 8.** Sinkage comparison.

From Figures 6–8, can be observed that resistance is predicted very well and the average error through all the speed range is 1.84%. For the dynamic trim, the average difference is 6.87%, but the EFD and CFD curves are perfectly aligned with constant offset. In absolute values, the maximum difference is 0.63 deg at  $Fr = 0.80$ , where the hull has its maximum trim of 6.26 deg. The average difference for sinkage is 6.94% and it can be seen from Figure 8 that, globally, it has a good agreement, but for some points at low  $Fr$ , it shows larger differences.

Even though the experiments are reliable for the total resistance measurement, the transfer to the full scale and correct power prediction of planing boats requires a precise assessment of the dynamic wetted surface. This value is possible to assess from experiments only as a further analysis of the underwater photography or photography of the transparent model bottom. Since Savitsky's work [10], the ship–model correlation was based on the simple approach of a prismatic (monohedral) hull and Savitsky's formula for the projected wetted pressure area. If the wetted lengths on the chine and on the keel are known, then the pressure area can be easily determined. In 2006, [30] proposed the distinction of the pure pressure area and whisker spray area calculated assuming the angle of separation as double as the angle of pressure area. This concept was discussed, and further contribution has been provided in [8] where it has been shown how this angle of separation of the whisker spray area depends on the deadrise angle. Work [30] is always based on the assumption of the full planing where the walls are completely dry, while in [8] the values are obtained for the  $Fr$  range 0.2–1.5, thus also including non-fully-planing conditions. It is important to highlight that the uncertainty of this "measurement" depends on the photography quality and subsequent postprocessing. It is not often discussed and remains relatively large with respect to other directly measured values, such as resistance, trim and sinkage, and in this case, it was not performed.

It is evident that for these not easily measurable parameters, the use of CFD is intrinsically advantageous because the pressure and viscous contributions are calculated separately, the wetted lengths and dynamic wetted surface are one of the first results of the calculations and the transfer to ship scale is straightforward.

Therefore, the numerical results have been further analyzed to report the wetted lengths and wetted surface in the whole speed range. The visualization in ParaView© is performed using the free surface 3D obtained with an iso value of 0.5 for the  $\alpha_{water}$  field and the hull pressure distribution. An example of the data elaboration in ParaView©, together with the photo from the towing tank at  $Fr = 1.96$ , is provided in Figure 9. The

obtained values of the dynamic wetted surface are summarized graphically in Figure 10, while the wetted lengths on the keel, chine and whisker spray on chine are reported in Figure 11 for the whole range of Froude numbers.



**Figure 9.** Example of dynamic wetted surface and wetted length analysis at  $Fr = 1.96$ . (a) Experimental; (b) numerical. For the numerical data only: wetted keel length (white), wetted chine length (green) and whisker spray length (red).

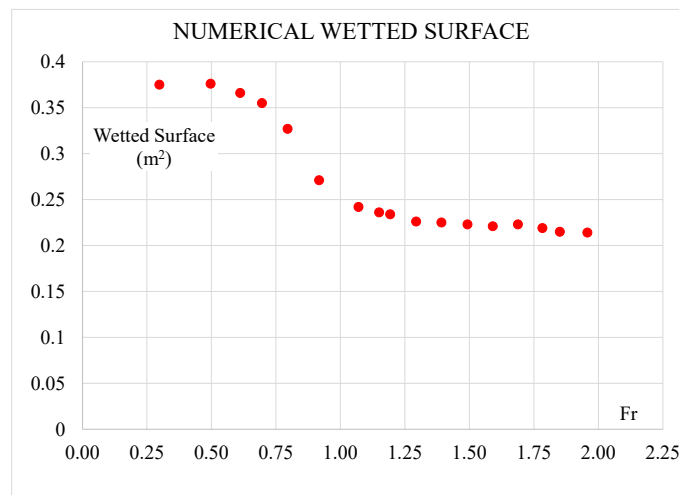


**Figure 10.** Numerical results for the dynamic wetted surface.

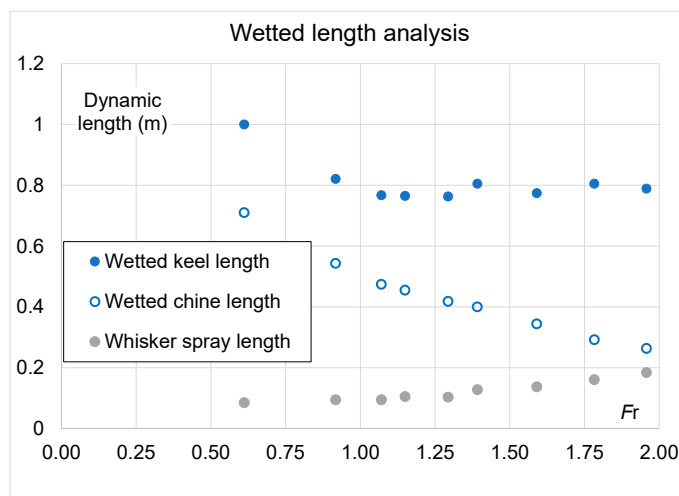


**Figure 11.** Numerical results for the wetted length at the chine and keel.

#### 4.2. Measured vs. Calculated Results in Regular Waves

For the seakeeping behavior of planing hulls, as characterized by the strong nonlinear phenomena, the simplest approach of comparing the RAO of the first harmonic of response and wave is not optimal. In [14,31,32] authors used the spectral analysis and showed not only the RAO as the first harmonic but also the super-harmonics of pitch and accelerations.

In this work, the comparison, as the first step in the seakeeping calculations by LincoSim, of only the time series has been analyzed in detail. In Figures 12 and 13, a sample of 4 s of the time series of the EFD and CFD is shown, at  $Fr = 0.99$  and  $1.49$ , respectively. In both figures, the comparison of the EFD (red lines) and CFD (blue lines) data is provided for selected quantities: encounter wave, heave, pitch on the left side and acceleration at CG and at bow position on the right side.

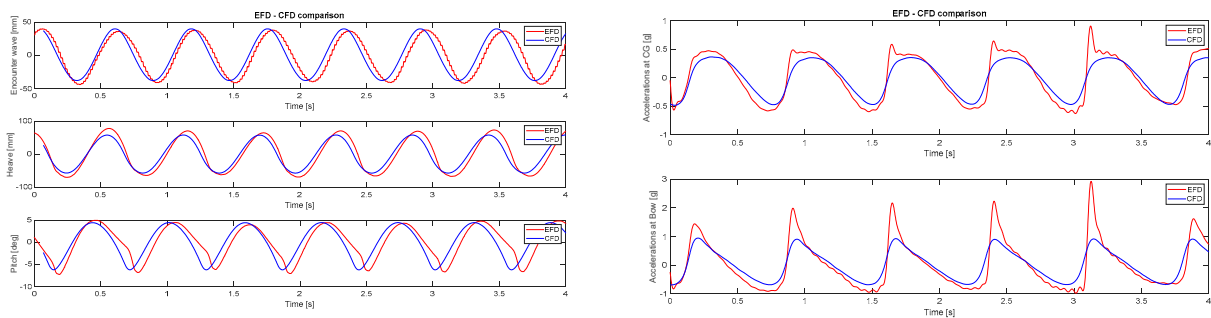


Figure 12. Comparison of measured (red) and simulated (blue) P43 planing hull in wave at  $Fr = 0.99$ .

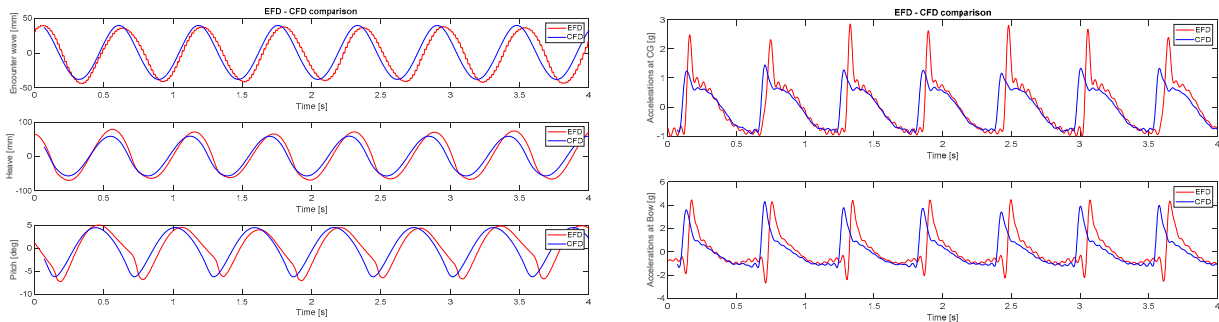


Figure 13. Comparison of measured (red) and simulated (blue) P43 planing hull in wave at  $Fr = 1.49$ .

The very good prediction of the heave and pitch can be observed at both speeds. For the acceleration prediction, the trend is perfectly matched, although it can be observed that the numerical values are smoother and little bit lower at both positions. For the acceleration results at higher speed, it can be seen how a small difference in position (experimental results at 0.47 m and CFD results at 0.39 m from stern) influences the motion composition and development of nonlinear responses. For the bow accelerations, extremely good matching is obtained, even a small vibration in the phase after impact is observed in the numerical results. Future work from the experimental side will face a wide range of wave frequencies to validate the LincoSim platform. The overall conclusions for these very first steps are that the results are very promising, as the observed differences between numerical and experimental data for heave and pitch are within a few percents, aligned with the results of [14,32,33]. More importantly, the simulation monitored output for the accelerations can spot the presence of multiple frequencies instead of just the one related to the regular encounter wave signal, thus confirming the ability of CFD simulation to account for relevant nonlinear responses of the ship while planing.

## 5. Conclusions

A validation of the LincoSim platform performed for the planing powerboat model up to the ship velocity of 40 knots is performed and reported. The simulations in calm water are performed in the length-based Froude number range from 0.3 to 2.0, extending what has been published so far using the LincoSim virtual towing tank.

The average differences in a whole speed range between CFD and EFD for the calm water simulations are 1.84%, 6.87% and 6.94% for resistance, dynamic trim and sinkage, respectively. These values are in line with the results reported in state-of-the-art works, where it was underlined how small differences in the hull geometry, ballasting conditions, and tow point location can have significant effects on the running trim predicted by CFD. From the visual observation of the photos from the experiments and analysis of wetted length on chine and spray length on chine, CFD simulations accurately describe the phenomenon, as confirmed by the excellent agreement of the total resistance.

A preliminary set of results for a seakeeping test in regular waves at two speeds,  $Fr = 0.99$  and  $1.49$  (20 and 30 knots in ship scale), for a selected wavelength defined by  $\lambda/L = 3.56$  is provided. The seakeeping analyses performed herein showed that automated CFD simulations can match experimental data, highlighting the complex nonlinear hull/wave interactions of the planing crafts. More precisely, in both the CFD and EFD output datasets, multiple frequencies can be spotted for the acceleration dynamics at given hull points. Even if not fully validated yet, the seakeeping workflow presented for the first time herein is promising in this regard. Deeper investigations of this nonlinear behavior are outside of the scope of the present preliminary test, and they will be analyzed in a future wider work.

The overall results presented here confirm the maturity of standardized and automated CFD modeling for hydrodynamic analysis of planing hulls in the whole speed range investigated. This approach has been tested and validated for only the model scale; nevertheless, considering the research applications for full-scale CFD models, like [26], we are looking forward to having a better understanding of its applicability for full-scale CFD modeling.

This synergic interplay of EFD and CFD can link the advantages of both methods to support hull design but also requires experiment planning and final data analysis to obtain physical parameters not easily measurable in laboratories.

**Author Contributions:** Experiments design, E.B. and C.B.; software development, R.P. and F.S.; writing—original draft, review and editing, editing and formal analysis, E.B., C.B., R.P. and F.S.; data curation, E.B. and R.P. All authors have read and agreed to the published version of the manuscript.

**Funding:** This research received no external funding.

**Data Availability Statement:** Data are contained within the article.

**Acknowledgments:** The e-SHyIPS project received funding from the Fuel Cells and Hydrogen 2 Joint Undertaking (now Clean Hydrogen Partnership) under grant agreement No. 101007226. This Joint Undertaking received support from the European Union's Horizon 2020 Research and Innovation programme, Hydrogen Europe and Hydrogen Europe Research.

**Conflicts of Interest:** The authors declare no conflicts of interest.

## References

1. Park, S.; Wang, Z.; Stern, F.; Husser, N.; Brizzolara, S.; Morabito, M.; Lee, E. Single- and two-phase CFD V&V for high-speed stepped planing hulls. *Ocean Eng.* **2022**, *261*, 112047.
2. Cui, L.; Chen, Z.; Feng, Y.; Li, G.; Liu, J. An improved VOF method with anti-ventilation techniques for the hydrodynamic assessment of planing hulls-Part 2: Applications. *Ocean Eng.* **2021**, *237*, 109505. [[CrossRef](#)]
3. Avci, A.G.; Barlas, B. Investigation of the optimum longitudinal single transverse step location for a high-speed craft. *Brodogradnja* **2023**, *74*, 47–70. [[CrossRef](#)]
4. Lee, E.J.; Mousaviraad, M.; Weil, C.R.; Jiang, M.J.; Fullerton, A.M.; Stern, F. Assessment of experiments and CFD for the semi-planing R/V Athena Model in calm water. *Ocean Eng.* **2021**, *236*, 109254. [[CrossRef](#)]

5. Judge, C.; Mousaviraad, M.; Stern, F.; Lee, E.; Fullerton, A.; Geiser, J.; Schleicher, C.; Merrill, C.; Weil, C.; Morin, J.; et al. Experiments and CFD of a high-speed deep-V planing hull—Part I: Calm Water. *Appl. Ocean. Res.* **2020**, *96*, 102060. [[CrossRef](#)]
6. Salvadore, F.; Ponzini, R. LincoSim: A Web Based HPC-Cloud Platform for Automatic Virtual Towing Tank Analysis. *J. Grid Comput.* **2019**, *17*, 771–795. [[CrossRef](#)]
7. Ponzini, R.; Salvadore, F.; Begovic, E.; Bertorello, C. Automatic CFD analysis of planing hulls by means of a new web-based application: Usage, experimental data comparison and opportunities. *Ocean Eng.* **2020**, *210*, 107387. [[CrossRef](#)]
8. Begovic, E.; Bertorello, C. Resistance assessment of warped hullform. *Ocean Eng.* **2012**, *56*, 28–42. [[CrossRef](#)]
9. Salvadore, F.; Ponzini, R.; Duque, J.H.; Reinaldos, C.A.; Soler, J.M. CFD analysis of a multiplatform catamaran by means of a web-based application: Experimental data comparison for a fully automated analysis process. *Appl. Ocean. Res.* **2021**, *116*, 102886. [[CrossRef](#)]
10. Savitsky, D. Hydrodynamic design of planing hulls. *Mar. Technol.* **1964**, *1*, 71–95. [[CrossRef](#)]
11. Hoggard, M.; Jones, M. Examining pitch, heave and accelerations of planing craft operating in a seaway. In Proceedings of the High-Speed Surface Craft Exhibition and Conference, Brighton, UK, 24–27 June 1980.
12. Blount, D.L. (Ed.) *Performance by Design—Hydrodynamics for High-Speed Vessels*; Printed in the USA; Donald L. Blount: Chesapeake, VA, USA, 2014; ISBN 0-978-9890837-1-3.
13. Zarnick, E.E. *A Nonlinear Mathematical Model of Motions of a Planing Boat in Regular Waves*; David Taylor Naval Ship Research and Development Center: Bethesda, MD, USA, 1978.
14. Rosen, A.; Garme, K.; Razola, M.; Begovic, E. Numerical modelling of structure responses for high-speed planing craft in waves. *Ocean. Eng.* **2020**, *217*, 107897. [[CrossRef](#)]
15. Tavakoli, S.; Bilandi, R.N.; Mancini, S.; De Luca, F.; Dashtimanesh, A. Dynamic of a planing hull in regular waves: Comparison of experimental, numerical and mathematical methods. *Ocean. Eng.* **2020**, *217*, 107959. [[CrossRef](#)]
16. Taunton, D.J.; Hudson, D.A.; Shenoi, R.A. Characteristics of a Series of High Speed Hard Chine Planing Hulls—Part II: Performance in Waves. *Int. J. Small Craft Technol.* **2011**, *153*, B1–B22.
17. Soletic, L. Seakeeping of a systematic series of planning hulls. In Proceedings of the 2nd Chesapeake Power Boat Symposium, Annapolis, MD, USA, 19–20 March 2010.
18. De Luca, F.; Pensa, C. The Naples Systematic Series—Second part: Irregular waves, seakeeping in head sea. *Ocean. Eng.* **2019**, *194*, 106620. [[CrossRef](#)]
19. Perić, R.; Abdel-Maksoud, M. Generation of free-surface waves by localized source terms in the continuity equation. *Ocean Eng.* **2015**, *109*, 567–579. [[CrossRef](#)]
20. Bertorello, C.; Oliviero, L. Hydrodynamic resistance assessment for not monohedral planing hull form. In Proceedings of the IMAM 2009 13th International Congress of International Maritime Association of Mediterranean, Istanbul, Turkey, 12–15 October 2009; Volume 2, pp. 703–707; ISBN 978-975-561-355-0.
21. Begovic, E.; Bertorello, C. Experimental Assessment of Seakeeping Characteristics for Non-Monohedral Planing Hulls. In Proceedings of the IMAM 2009, 13th International Conference Towards the Sustainable Marine Technology and Transportation, Istanbul, Turkey, 12–15 October 2009; Volume 3, pp. 927–933; ISBN 978-975-561-355-0.
22. Fossati, F.; Muggiasca, S.; Bertorello, C. Aerodynamics Of High Speed Small Craft. In Proceedings of the FAST 2013—12th International Conference on Fast Sea Transportation, Delft, The Netherlands, 2–5 December 2013.
23. Begovic, E.; Bertorello, C.; Pennino, S.; Piscopo, V.; Scamardella, A. Statistical analysis of planing hull motions and accelerations in irregular head sea. *Ocean Eng.* **2016**, *112*, 253–264. [[CrossRef](#)]
24. Wang, Z.; Stern, F. Moving Contact Line and No-Slip Boundary Conditions for High-Speed Planing Hulls. In Marine 2023. Available online: [https://www.scipedia.com/public/Wang\\_Stern\\_2023a](https://www.scipedia.com/public/Wang_Stern_2023a) (accessed on 25 April 2024).
25. Menter, F.; Carregal Ferreira, J.; Esch, T.; Konno, B.; Germany, A.C. The sst turbulence model with improved wall treatment for heat transfer predictions in gas turbines. In Proceedings of the International Gas Turbine Congress, Tokyo, Japan, 2–7 November 2003; pp. 2–7.
26. Huang, L.; Pena, B.; Thomas, G. Towards a full-scale CFD guideline for simulating a ship advancing in open water. *Ship Technol. Res.* **2023**, *70*, 222–238. [[CrossRef](#)]
27. Perić, R.; Vukčević, V.; Abdel-Maksoud, M.; Jasak, H. Optimizing wave generation and wave damping in 3D-flow simulations with implicit relaxation zones. *Coast. Eng.* **2022**, *171*, 104035. [[CrossRef](#)]
28. Python Code for Optimal Lambda Computation. Available online: <https://github.com/wave-absorbing-layers/relaxation-zones-for-free-surface-waves> (accessed on 30 April 2024).
29. Manual Usage of the Python Code for Optimal Lambda Computation. Available online: <https://usermanual.wiki/Document/Manual.2128294547.pdf> (accessed on 30 April 2024).
30. Savitsky, D.; De Lorme, M.F.; Datla, R. Inclusion of “Whisker Spray” Drag in Performance Prediction Method For High-Speed Planing Hulls. *Mar. Technol. SNAME News* **2007**, *44*, 35–56. [[CrossRef](#)]
31. Begovic, E.; Bertorello, C.; Pennino, S. Experimental Seakeeping Assessment of a Warped Planing Hull Model Series. *Ocean. Eng.* **2014**, *83*, 1–15. [[CrossRef](#)]

32. Capasso, S.; Tagliafierro, B.; Mancini, S.; Martinez-Estevéz, I.; Altomare, C.; Dominguez, J.M.; Viccione, G. Regular Wave Seakeeping Analysis of a Planing Hull by Smoothed Particle Hydrodynamics: A Comprehensive Validation. *Mar. Sci. Eng.* **2023**, *11*, 700. [[CrossRef](#)]
33. Samuel, S.; Mursid, O.; Yulianti, S.; Kiryanto, K.; Iqbal, M. Evaluation of interceptor design to reduce drag on planing hull. *Brodogradnja* **2022**, *73*, 93–110. [[CrossRef](#)]

**Disclaimer/Publisher’s Note:** The statements, opinions and data contained in all publications are solely those of the individual author(s) and contributor(s) and not of MDPI and/or the editor(s). MDPI and/or the editor(s) disclaim responsibility for any injury to people or property resulting from any ideas, methods, instructions or products referred to in the content.